This manuscript was published as formal in:

International Journal of Biological Macromolecules 2020, 160, 398-408

DOI: 10.1016/j.ijbiomac.2020.05.207

https://doi.org/10.1016/j.ijbiomac.2020.05.207

***Title*:**

New formulations based on salicyl-imine-chitosan hydrogels for prolonged drug release

Manuela-Maria Iftime[1]*, Liliana Mititelu Tartau[2], Luminita Marin[1]

[1] “Petru Poni” Institute of Macromolecular Chemistry, Grigore Ghica Voda Alley, Iasi, Romania

[2] “Gr. T. Popa” University of Medicine and Pharmacy, Iasi, Romania

*ciobanum@icmpp.ro

Abstract

The objective of this paper was to investigate the new formulations based on salicyl-imine-chitosan hydrogels as potential controlled drug release systems. They were prepared by *in situ* hydrogelation of chitosan with salicylaldehyde in the presence of diclofenac sodium salt (***DCF)*** as model drug. FTIR, X-ray Spectroscopy, POM and SEM techniques were used to confirm the structural, supramolecular and morphological particularities of the formulations. Swelling test, *in vitro* enzymatic biodegradation and release profile were investigated in similar conditions mimicking the *in vivo* environment, and the release mechanism was assessed by fitting into five mathematical models. It was established that the formulations have the capacity to release ***DCF*** in a sustained manner for 10 days rate, the drug release rate being correlated to the crosslinking density and hydrogelation speed. The biodegradation occurred in three main stages, reaching a mass loss of 48 % after 21 days. In order to be used in the biomedical field, the *in vivo* biocompatibility of the formulations was investigated on experimental rats. After 7 days of subcutaneous implantation, no influence on the hematologic profile, liver, kidney or immune defence capacity were observed, suggesting these formulations as valuable materials for biomedical devices.

Keywords: hydrogels, chitosan, salicylaldehyde, diclofenac sodium salt, prolonged release, biocompatibility

1. Introduction

In recent years, researchers are focusing on developing new materials which can be used as local therapy alternative, to load and release various drugs or biologically active species. The ideal materials for these formulations need to release the entrapped drug at the required site, at stipulated times, in response to specific physiological stimuli [1]. The literature data over last years revealed that numerous efforts were carried out to develop newer materials for application in the controlled drug release, using different approaches such as chemical [2] and physical modification or blends of polymers [3-5]. The advantages of such controlled release systems over the conventional dosage forms, mainly consist in minimizing the gastric irritant side effects [4]. The most valuable materials for such applications proved to be those originating from natural resources, such as cellulose, chitosan, gelatin, gellan gum [5] pectin, collagen and peptides [6,7]. In order to increase the bioactivity of the natural macromolecules, different type of modifications were studied and reported. Among them, hydrogels are a promising alternative, due to their good capacity to absorb various fluids and to swell, reaching hydrodynamic properties similar to those of biological tissues [8]. For drug delivery

applications, they can be used in different forms (e.g. creams, patches, or tablets) for oral administration, injection and transdermal delivery [9]. Among the multitude of natural polymers, the cationic polysaccharide chitosan has a special role as carrier for various bioactive molecules, due to its physico-chemical, biocompatible and biodegradation properties. The polycationic nature of chitosan is an important property that enhances the formation of complexes with different anionic drugs (diclofenac, cefadroxil, ofloxacin, bevacizumab and so on) favoring the smoother dispersion [10]. By crosslinking of chitosan with different physical or chemical agents, various materials were obtained, which are capable to entrap a variety of drugs and release them in a controlled manner [11-13] An important research direction was dedicated to the chitosan modification in order to improve its delivery potential while physico-chemical and bio-chemical properties are preserved. These changes targeted the improvement of the biodistribution and retention of drugs, and led to a large variety of chitosan derivatives with specific properties for different areas of drug administration [14-16]. It was demonstrated that crosslinking with various agents can adjust the morphology and viscoelastic properties, improving the potential of chitosan-based hydrogels to act as a matrix for drugs [17]. The research activity of our group evidenced the possibility to obtain hydrogels based on chitosan and different natural monoaldehydes with good properties for bioapplications: biocompatibility, mechanical strength, biodegradability, thixotropy, high drug-loading capacity, and its controlled release [18-26]. The use of the monoaldehydes introduced the advantage of higher biocompatibility and lower cytotoxicity compared to other crosslinking reagents such as glutaraldehyde, formaldehyde, and epoxy compounds [19]. Salicylaldehyde, a natural aldehyde occurring in buckwheat [27], proved to be an excellent crosslinker for chitosan. The hydrogels prepared from chitosan and salicylaldehyde revealed excellent thixotropic and self-healing properties [18], suggesting their capability to act as matrix for drug delivery systems. To demonstrate the feasibility of this newly developed chitosan-based hydrogel to act as a matrix for sustained release of drugs, formulations encapsulating diclofenac sodium salt (***DCF***) were prepared and evaluated. Diclofenac sodium salt (an anti- inflammatory non-steroidal drug used in general in the treatment of rheumatoid arthritis) was chosen as a model drug, starting from the hypothesis that there are many scientific publications devoted to the ***DCF*** containing systems [3, 28-37]. This will contribute to a proper comparative evaluation of the drug delivery properties, allowing estimating the value of the new hydrogels as drug matrix. The gelation time, swelling behaviour, *in vitro* biodegradability, *in vitro* drug release and *in vivo* biocompatibility were evaluated.

2. Experimental Part

2.1. Materials

Low molecular weight chitosan, (193 kDa, degree of deacetylation 82%, Aldrich); salicylaldehyde (SA) (98%), ethanol, glacial acetic acid, phosphate buffer (PBS) (pH=7.4), diclofenac sodium salt (***DCF***), lysozyme (lyophilized powder, protein 90 %, 40 000 units/mg protein) were purchased from Aldrich and used as received.

2.2. Preparation of DCF-loaded chitosan-salicyl-imine hydrogels (CSDx)

A series of four formulations were prepared by *in situ* hydrogelation of chitosan with salicylaldehyde in the presence of ***DCF***. The four formulations have different crosslinking degrees, reached by varying the molar ratio between the glucosamine units of chitosan and salicylaldehyde. They were coded **CSD1-CSD3 (CSDx)**, the number reflecting the molar ratio of the functional groups (Table 1). Briefly, corresponding amounts of chitosan were dissolved into 0.7% acetic acid solution under stirring at 55^{o}C, to give a 2% solution. Subsequently, a solution of salicylaldehyde (SA) and diclofenac sodium salt (***DCF***) in ethanol (1%, w/v) was added to the chitosan, and maintained 3 hours in these conditions. The ***DCF*** amount was kept constant related to the dry mass of the final drug system (2.4 %, w/w). Reference hydrogels (without drug, namely **CS1-CS3** (**CSx**)) were prepared using similar molar ratios of the functional groups and preparation conditions (Table 1).

Table 1. Composition of the formulations (**CSD1-CSD3**) and references (**CS1-CS3**)

Code	NH_2/CHO	Chitosan (mg)	SA (mg)	***DCF*** (mg)	Gelation time (min)	Xerogels (mg)
CSD1	1/1	38.04	22.46	1.5	1	62
CSD1.5	1.5/1	43.40	17.1	1.5	3	62
CSD2	2/1	46.71	13.79	1.5	15	62
CSD3	3/1	50.55	9.95	1.5	*	62
CS1	1/1	38.04	22.46	-	2	60.5
CS1.5	1.5/1	43.40	17.1	-	4	60.5
CS2	2/1	46.71	13.79	-	60	60.5
CS3	3/1	50.55	9.95	-	**	60.5

* a viscous opalescent liquid was observed after one day; ** a viscous liquid that still flew after two weeks

In the case of the formulations, the hydrogelation occurred over 1-3 minutes for the systems with higher amount of salicylaldehyde (**CSD1, CSD1.5**) and after 15 minutes for **CSD2**. In the case of the **CSD3** sample, a viscous opalescent liquid formed and this aspect was maintained over 24 hours, the visual hydrogelation being not observed. In the case of the reference hydrogels, the hydrogelation was observed after 2-4 minutes for **CS1** and **CS1.5**; 1 hour for **CS2**, while the **CS3** transformed into a viscous liquid which still flew after two weeks.

Excepting **CSD3** sample, all the formulations appeared as transparent yellowish semisolid materials, with smooth texture, similar to the reference hydrogels (Fig. 1). Further, all the formulations and reference hydrogels were kept uncovered over 14 days until the initial volume of chitosan solution was reached and then they were subjected to lyophilisation in order to obtain the corresponding xerogels. The formulation xerogel prepared with the largest amount of salicylaldehyde (**CSD1**) was brittle and had a heterogeneous appearance, while those with a lower amount (**CSD1.5**, **CSD2** and **CSD3**) were homogeneous, with a porous aspect. For FTIR, X-ray, biodegradation, biocompatibility and drug release tests, certain amounts of xerogels were manufactured as round pellets with a hydraulic press at 2 N/m^2.

2.3. Characterization

2.3.1. Lyophilization. The dry state of the formulations and reference hydrogels were obtained by freezing in liquid nitrogen and further subjected to lyophilization to give the corresponding xerogels, using a LABCONCO Free Zone Freeze Dry System equipment, at -50 ^oC and 1.510 mbar, for 24 hours.

2.3.2. Fourier transformed infrared spectroscopy (***FTIR***). ATR-FTIR spectra were registered on a FTIR Bruker Vertex 70 Spectrophotometer equipped with a ZnSe single reflection ATR accessory. The registration was performed in the 600–4000 cm^{-1} spectral range, with 32 scans at 4 cm^{-1} resolution. The overlapped and hidden peak positions of the 1600 – 1500 cm^{-1} region in the FTIR spectrum of the series CSDx were determined with the second derivative of the spectrum. The stretching vibration regions were deconvoluted by a curve-fitting method, and the areas were calculated with a 50 % Lorentzian and 50 % Gaussian function. The curve-fitting analysis was performed with the OPUS 6.5 software and OriginProBit9. The procedure led to a best fit of the original curve with an error of less than 0.004.

2.3.3. Wide angle X-ray diffraction (WXRD) was performed on a Bruker D8 Advance diffractometer with Ni-filtered Cu-Kα radiation (λ = 0.1541 nm), range of 2 ÷ 40° range 2θ° (2 theta), at room temperature. The dimension of the imine clusters (D) was calculated applying the Debye–Scherrer formula for the reflection peak around 6^o: $D = K\lambda/\beta\cos\theta$, where D is the average diameter in nm, k is the shape factor (k¼=0.9); λ is the X-ray wavelength; β is the full width at half maximum of the diffraction in radians, and θ is Bragg's diffraction angle [38].

2.3.4. The morphology was investigated with a field emission ***Scanning Electron Microscope*** (SEM) EDAX – Quanta 200 at accelerated electron energy of 20 KeV. The size of pores was calculated using Image J program.

2.3.5. The ordered state of the xerogels was evidenced by **polarized light microscopy (POM)** with a Leica DM 2500 microscope.

2.3.6. The in vitro release was completed in experimental conditions mimicking the tissue medium, such as: phosphate buffer (PBS) of pH=7.4 at 37^{o}C. The experimental procedure was as follows: pellets of xerogels of 62 mg were dipped into vials containing 10 mL of PBS. At certain moments, 2 mL aliquots were withdrawn and replaced with fresh buffer. The ***DCF*** amount in the aliquots samples was determined by recording the characteristic absorption band at 275 nm, and fitting its absorbance on a predetermined calibration curve [23]. The UV-Vis spectra were registered on an UV-visible spectrophotometer (Perkin Elmer, Lambda 10). The cumulative release of the ***DCF*** was calculated using equation: % ***DCF*** = $[(10C_n + 2\Sigma C_{n-1})/m_o]$ x 100, where C_n and C_{n-1} represent the concentrations of the drug in the supernatant after n and n-1 withdrawing steps, respectively, and m_o = 1.5 mg, corresponding to the ***DCF*** loaded in the hydrogels. In order to evaluate ***the mechanism of the DCF release from the formulations***, the data were fitted on a series of equations of mathematical models, such as: *Korsmeyer-Peppas, Zero order, First order, Higuchi and Hixson-Crowell* [23, 39, 40].

2.3.7. The swelling behaviour of the formulations was investigated by immersing pellets of 62 mg in 10 mL phosphate buffered solutions (PBS; pH=7.4) at 37^{o}C till equilibrium. The mass equilbrum (MES) was determined with equation eq.1:

$$MES=W_s\text{-}W_d/W_d; \quad (1)$$

where: W_s - the weight of the swollen sample; W_d- the weight of the dry sample [18,29].

2.3.8. **Enzymatic degradation.** The *in vitro* biodegradation of the formulations and reference hydrogels was determined gravimetrically and by SEM observation, on representative samples **(CS1.5, CS2** and **CSD2)**, in conditions mimicking physiological environment. Samples of ~8 mg were incubated in 8 mL of lysozyme solution in PBS (10 mg/L), at 37°C [23]. The lysozyme solution was refreshed every three days to simulate continuous enzyme activity. At specified time intervals, hydrogels were removed from the medium, washed with distilled water, lyophilised and further subjected to quantitative and qualitative analysis, by calculation of weight loss percentage, and acquiring SEM images, respectively. The weight loss percentage was calculated with eq.2:

$$\text{Weight loss (\%)} = 100 \times (W_i - W_t)/W_i \quad (2)$$

where, W_i and W_t, denote the initial weight and weight of the samples at predetermined times. The experiment was realized in triplicate. To proper attribute the intrinsic influence of the

lysozyme on the sample degradation, the biodegradation experiment was performed in the absence of lysozyme, in blank PBS medium, as well.

2.3.9. **In *vivo* biocompatibility**. The biocompatibility of the studied formulations was assessed *in vivo*, on experimental rats. For these experiments were used **CSD1.5** and **CSD2** pellet formulations of 62 mg containing 1.5 mg of ***DCF***, while the pristine **CS1.5** and **CS2** pellets of 60.5 mg were used as reference. The amount of ***DCF*** was in agreement with the pharmaceutical recommendations of the maximum dose per kg [23].

30 white male Wistar rats, weighing 150-200 g were used in the experiment. The animals were kept for 1 week before starting the study, in well-ventilated plastic cages in standard atmosphere (temperature of 22±1°C, a relative humidity of approximately 50%, and light/dark cycle of 12/12 hours) and maintained on a normal diet, with water *ad libitum*, except during the investigations. 2 hours prior the experiment, rats were positioned on a raised wire mesh, under a clear plastic box and allowed to adapt to the laboratory environment. The rats were divided into five groups consisting of six animals each. Each group was treated with pellets as follows: **CS1.5**, **CSD1.5**, **CS2** and **CSD2**. Rats with cotton pellets impregnated with the same dose of ***DCF*** were considered as positive control animals in the study. Each animal was anaesthetized (with 50 mg/kg body weight ketamine and 10 mg/kg body weight xylazine) and the pellets were inserted subcutaneously through a slight incision in one side in the dorsal region, which was thereafter sutured. The tested groups were kept under aseptic conditions for seven consecutive days.

During the experiment, the rats were weighted and the general status and the behavioural manifestations were examined. The *in vivo* biocompatibility estimation was based on the assessing of the hemodynamic, immune and biochemical profile of the animals, analysed at 1 and 7 days after the implantation. To do this, 0.3 ml of blood samples were taken from the lateral tail vein under topical anaesthesia with 1% benzocaine. The blood samples were collected in tubes containing ethylene-diamine-tetra-acetic acid (EDTA) and centrifuged (2000 rpm, 10 min, 4ºC) in a refrigerated centrifuge for serum separation [41]. The dynamics of biochemical modifications, the cellular and immunologic responses were estimated by monitoring the following parameters: differential white cell count, the serum alanine aminotransferase (ALT), aspartate aminotransferase (AST), lactate dehydrogenase (LDH), the plasma uric acid and creatinine, the phagocytic capacity of peripheral neutrophils (nitro-blue tetrazolium - NBT test) and the serum complement activity [42-44]. The data were expressed as the mean ± standard deviation (S.D.). The SPSS program, variant 17.0 for Windows and

ANOVA method were used to estimate the differences between the tested groups. The degree of statistical significance was set at *p* (probability) below 0.05.

The *in vivo experiments* were approved and performed in accordance with the recommendation of the „Grigore T. Popa“ University Commission for Research and Ethical Issues, regarding the handling and use of the experimental animals [45], in compliance with the international ethical normative of the European Directive 2010/63/EU. Each animal was used only once and was euthanized immediately at the end of the experiment [46, 47].

3. Results and discussion

The overall reaction for *in situ* encapsulation of a constant amount of diclofenac sodium salt in the hydrogels based on chitosan crosslinked with salicylaldehyde was represented in Fig. 1. Four formulations of drug carriers with different crosslinking density have been prepared by varying the molar ratio between glucosamine units of chitosan and aldehyde groups of salicylaldehyde (Table 1). As demonstrated in previous studies, the hydrogelation is expected to occur due to the self-ordering of the newly formed imine units into clusters playing the role of crosslinking nodes [18-26]. To prove that this non-classical hydrogelation take place in the presence of ***DCF*** as well, the formulations were investigated by FTIR, X-ray, SEM and POM techniques, and data were compared to those obtained for the reference hydrogels.

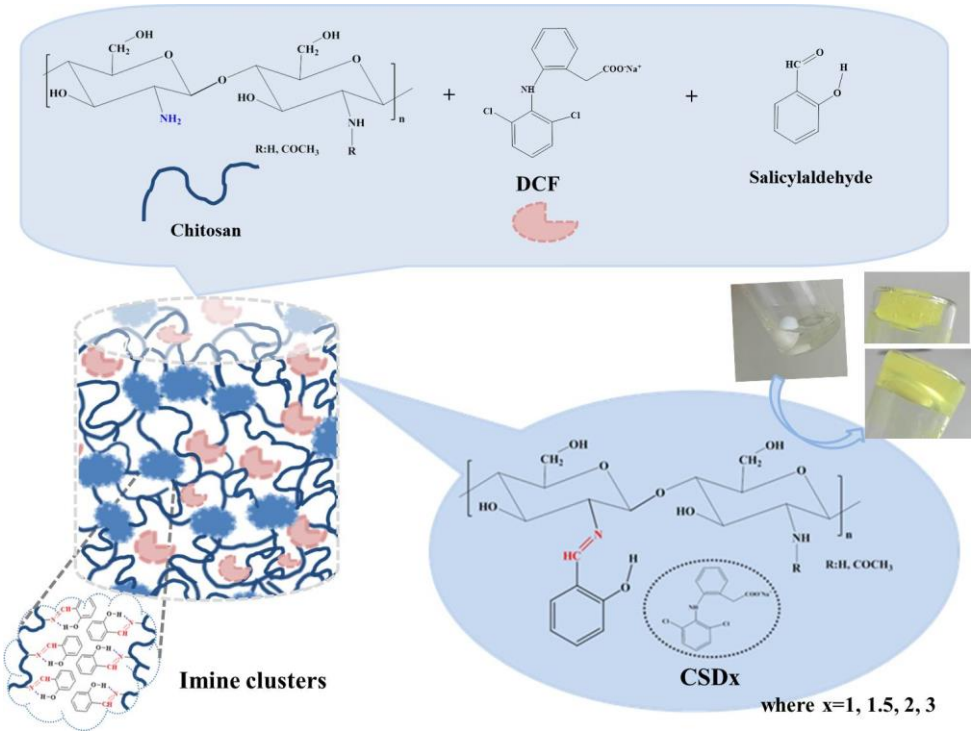

Fig.1. Schematic representation of the synthesis of the salicyl-imine-chitosan hydrogels *in situ* loaded with ***DCF***

3.1. Structural characterization by FTIR

The **CSD1-CSD3** formulations showed almost similar FTIR spectra to those of the corresponding **CS1-CS3** reference xerogels indicating that ***DCF*** didn't hinder the imine self-ordering process demonstrated for salicyl-imine-chitosan hydrogels (Fig. 2a, Fig. S1) [18].

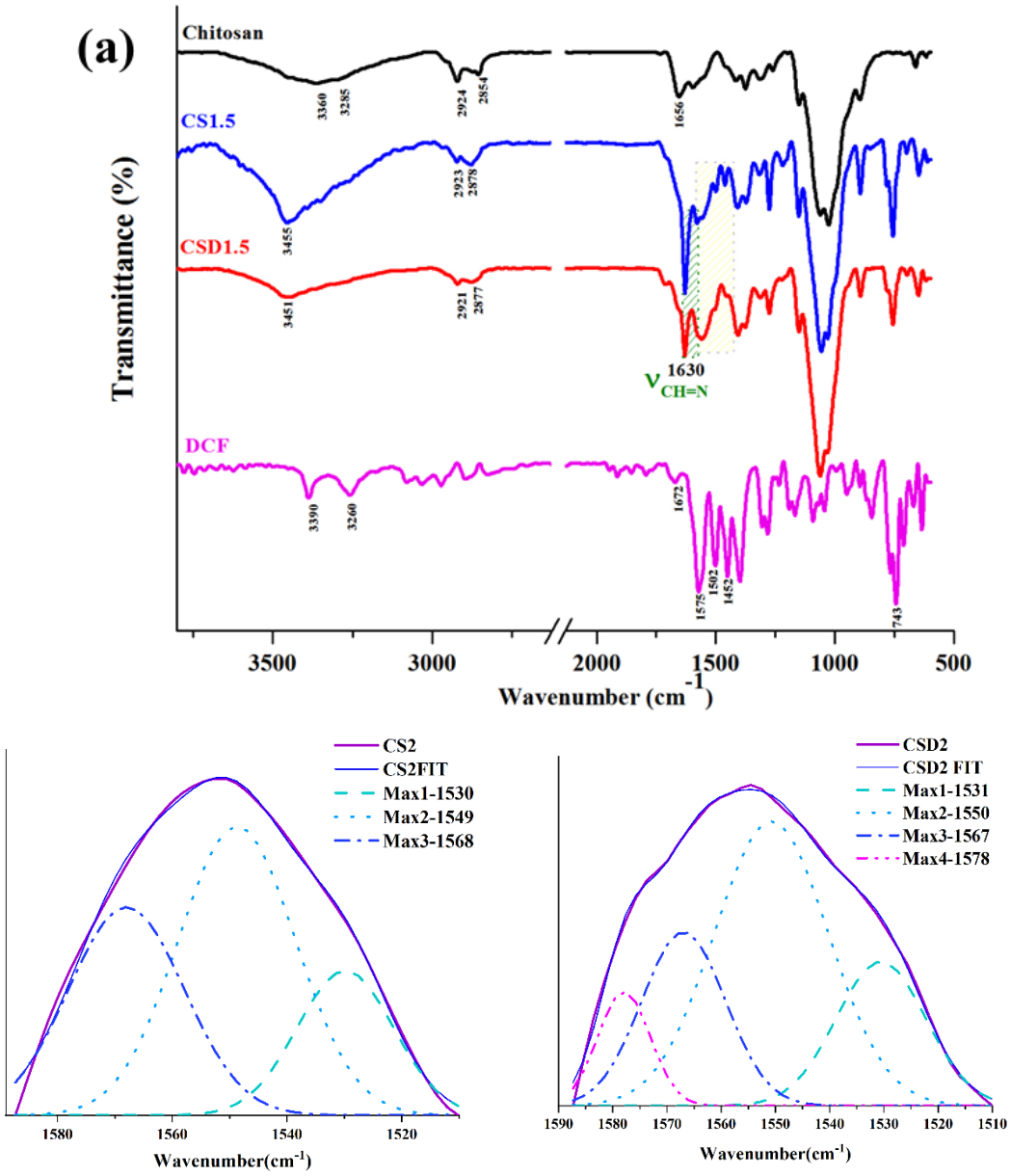

Fig. 2. a) Comparative FTIR spectra of the ***DCF***, **CSD1.5**, **CS1.5** and chitosan; b) deconvolution of the 1600-1500 spectral domain of CS2 and CSD2 samples

The distinctive peak that proves that the hydrogelation process occurred by forming the imine clusters it can be observed around 1630 cm^{-1}, for **CSx** and **CSDx**. The absorption band

characteristic for the hydrogen bond network was shifted to higher wavenumbers for both kind of samples (**CSx** and **CSDx**) compared to chitosan (from 3360 cm^{-1} for chitosan to 3455 cm^{-1} for **CSx** and 3451 cm^{-1} for **CSDx**), indicating a redistribution of the H-bonds as result of the hydrogelation process. The slight differences of the band maximum in **CSDx** compared to **CSx** suggest the contribution of the drug on the hydrogen bond network of the chitosan, the most probably by H-bonds between the carboxyl and secondary amine groups with hydroxyl and amine units. In the 1700-1452 cm^{-1} spectral domain of the CSDx formulations, the absorption bands characteristic to the DCF, such as: carboxyl stretching vibration (1575 cm^{-1}), C=C ring stretching (1502 cm^{-1}), CH_2 bending (1452 cm^{-1}) and HC-N-CH bending vibration (1502 cm^{-1}), appeared superposed with the vibration bands of the hydrogels matrix [48]. The deconvolution of the 1510-1590 broad band (Fig. 2b) revealed that the stretching vibration of the carboxyl unit has been shifted to higher wavenumbers (1578 cm^{-1}), the most probably due to hydrogen bond with the matrix. Overall, these spectral modifications of the vibration bands of CSDx spectra compared to the CSx, indicated the anchoring of the drug into the hydrogel matrix by physical interactions [11].

3.2. Supramolecular characterization by Wide Angle X-ray diffraction

Representative Wide Angle X-ray diffractograms for the reference hydrogels (**CS1.5**), ***DCF*** sodium diclofenac powder and formulations (**CSD1-CSD3**) are shown in Fig. 3. Investigation of the supramolecular architecture of the reference hydrogels demonstrated that crosslinking is the result of a self-ordering of the salicyl-imine units into 3D clusters. They were defined by inter-layer, inter-chain and inter-molecular distances, distinguished into diffractograms as a sharper reflection at 6.15-6.6º, and broader reflections at 14 and 20º (Table S1). All these reflections were present in the diffractograms of the **CSDx** formulations, demonstrating that the presence of ***DCF*** drug didn't suppress the hydrogelation process during the *in situ* encapsulation. This was also confirmed by the absence of significant alterations of the dimension of the imine clusters estimated by applying Debye–Scherrer equation to the reflection peaks characteristic to the inter-layer distance of the ordered imine clusters (Table S2) [38,49]. No clear reflections of the ***DCF*** drug were discriminated into diffractograms, suggesting that it was fine dispersed into the matrix, the most probably at submicrometric level. Comparing the obtained data with other formulations prepared by *in situ* encapsulation of ***DCF*** in hydrogels based on chitosan and monoaldehydes, it appeared that the slower gelation time favoured an advanced dispersion of the drug into the matrix [23, 50].

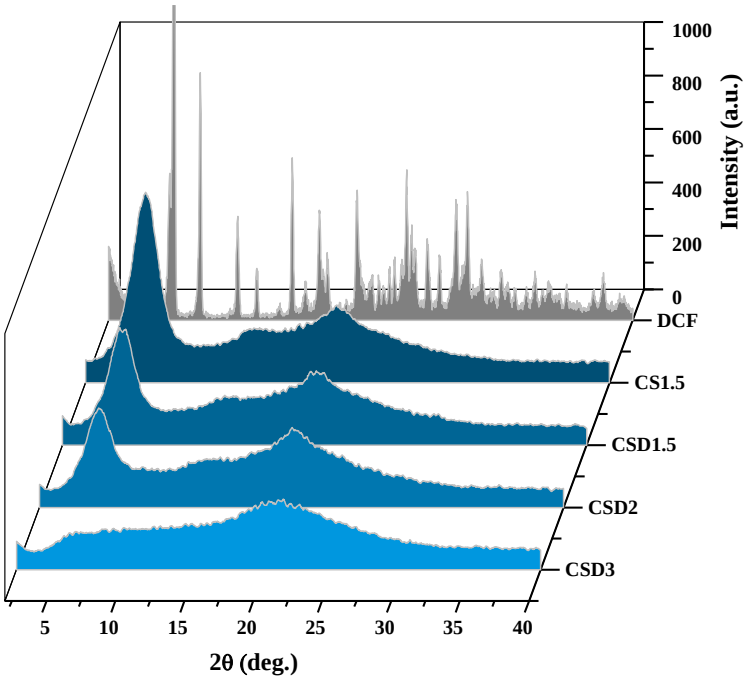

Fig.3. The X-ray diffractograms of pure ***DCF*** and some representative formulations and a reference

3.3. Morphology of the drug delivery systems

Typical SEM photographs of the formulations and corresponding reference hydrogels were presented in Fig. 4. The formulations showed a porous morphology, once again confirming that ***DCF*** didn't affect the hydrogelation process. The pores were interconnected and their diameter progressively increased as the crosslinking degree decreased, respecting the general rule proved for many hydrogels [51-54]. Thus, while in the case of the **CSD1** formulation, with the highest crosslinking degree, the average diameter of the pores was around 7 μm (Fig.4a), in the case of **CSD3** (Fig.4d), with the lowest one, it reached a value around 35 μm. CSD1.5 and CSD2 displayed an average diameter around 10 and 15 μm, respectively. On the other hand, compared to the reference hydrogels, significant differences of pore dimensions appeared, indicating the interference of the drug on the crosslinking. Considering that no drug crystals were observed into the pores or on their walls, it can be estimated that this interference was given by the intermolecular forces developed between chitosan and drug, increasing the system viscosity. This resulted in an intimate dispersion of the drug into mixture, leading to its encapsulation into the pore walls at submicrometric level, fact indicated by X-ray diffractograms too. Further, polarized light microscopy (POM) was employed as a complementary method to X-ray diffraction and scanning electron microscopy techniques. The POM images showed continuous textures of strong birefringence, characteristic for ordered

phases (Fig. 4e,f,g,h and Fig. S3) [18, 55]. It can be seen that the strong birefringence was given by the pore walls, as better clarified for the formulations with large pores (Fig.4h). No obvious crystals of ***DCF*** drug were observed into the pores cavity. Compared to the reference hydrogels (Fig.4f), a more vivid coloured birefringence was remarked for the formulations (Fig. 4g), suggesting that the drug favoured a more advanced supramolecular ordering, possible due to the encapsulation of the drug molecules as spacers between the chitosan chains [23].

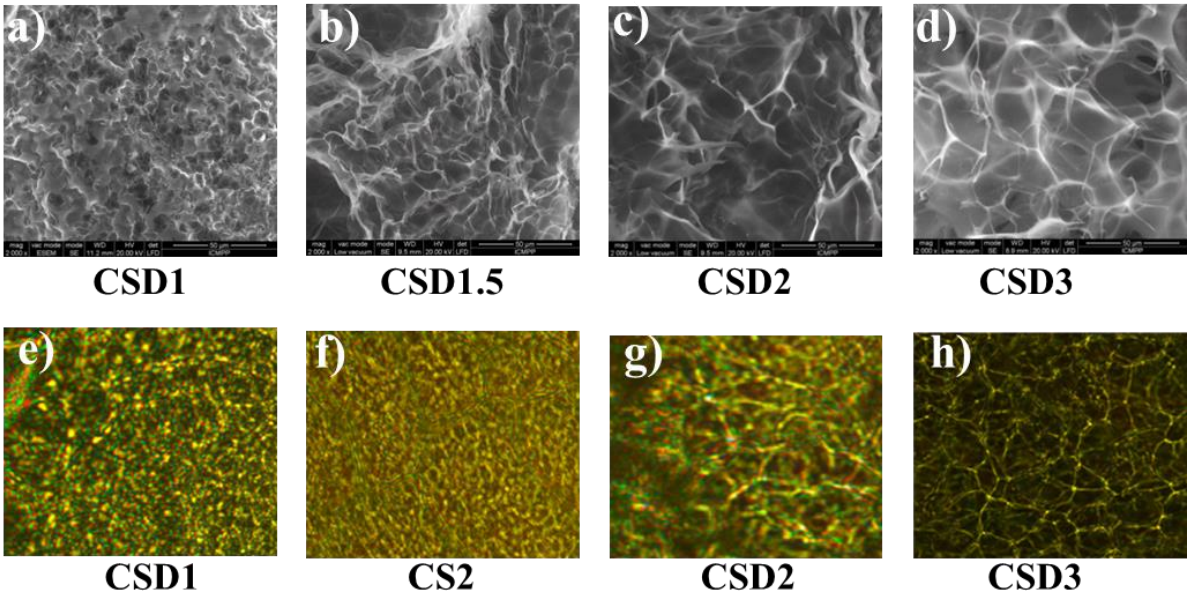

Fig.4. SEM and POM images of the formulations and the reference hydrogels

3.4. Swelling of the formulations

Taking into consideration that the swelling is a process which influences the rate of drug release, the mass equilibrium swelling (MES) and the swelling kinetic of the formulations and corresponding reference hydrogels were determined in similar conditions as those followed for *in vitro* drug release (PBS, 37^{o}C). The graphical representation of the swelling over time, for representative formulations and reference hydrogels (**CSD1.5** *versus* **CS1.5** and, **CSD2** *versus* **CS2**) showed that the presence of drug accelerated the swelling and prompted a significant MES increment, i.e. from 13 to 20, and from 16 to 28, respectively (Fig. 5). This can be easily explained considering that the drug release into the PBS produces defects into the salicyl-imine-chitosan matrix which favored the swelling. As expected, the MES was higher for a lower crosslinking degree. It should be noted that the MES was reached in less than two hours **[**14**]**.

3.5. *In vitro* enzymatic degradation

The biodegradation was investigated on representative formulations (**CSD2**, **CSD1.5**) in conditions mimicking the *in vivo* degradation environment, i.e. PBS enriched with

Lysozyme, as it is well known that chitosan is mainly degraded by this enzyme [56]. The enzyme concentration in PBS was similar to that found in human body, and over the investigation period it was refreshed to maintain it at this value. The degradation was monitored by measuring the mass loss over time and acquiring SEM images. A reference hydrogel was analyzed in similar conditions, in order to assess the role of drug encapsulation on biodegradation (**CS2**). To assess the intrinsic influence of the Lysozyme, the degradation process was also followed in blank PBS (**CS2P**).

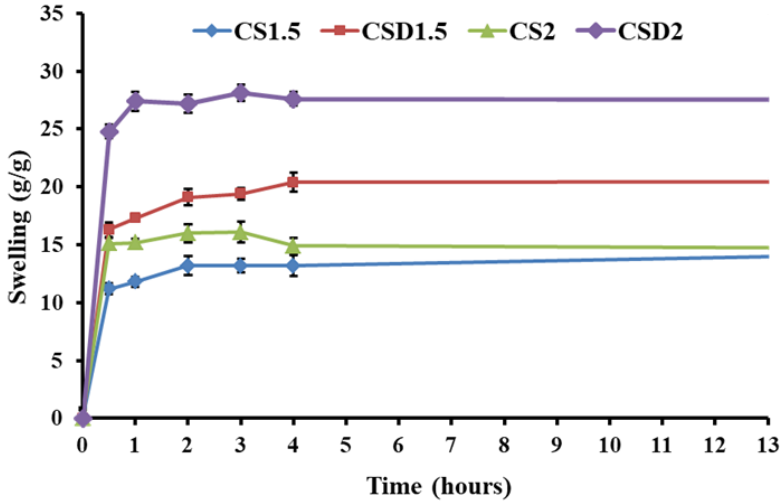

Fig. 5. Graphical representation of the swelling over time, for representative formulations and reference hydrogels

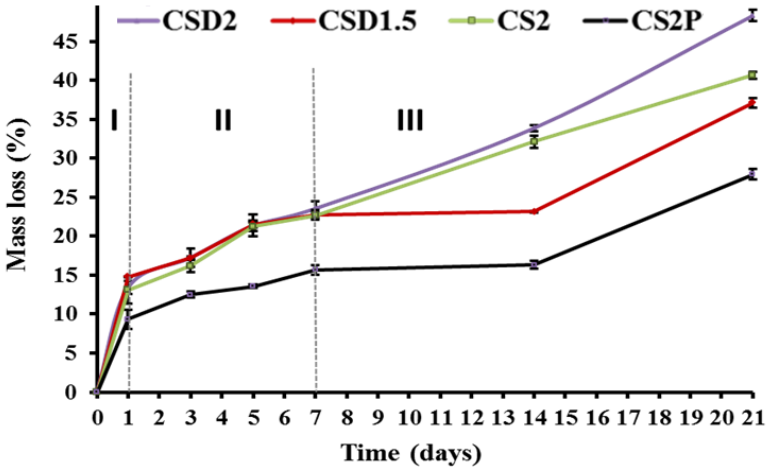

Fig. 6. *In vitro* biodegradation profiles of representative formulations and references. Triplicates of each sample were analysed (n=3), and each point represents the mean value ± standard deviation.

The mass loss profile was given in Fig. 6. At a first glance, can be remarked that (i) the biodegradation occurred in three stages of different degradation rates, and (ii) the enzymatic degradation rate is higher compared to that in PBS. Thus, the biodegradation massively

occurred in the first 24 hours, when a 12 % mass loss was reached in Lysozyme and 8 % in PBS (*stage I*). In the next 6 days the rate of mass loss was slower (an average of 1.2% per day), reaching 20 % in Lysozyme and 12 % in PBS (*stage II*). In the next 14 days, the rate of mass loss increased (at an average of 2% per day) reaching 48 % for **CSD2** in lysozyme and 25 % for **CS2P** in PBS, in day 21 (*stage III*). The mass loss of the reference hydrogel was slightly lower compared to that of the corresponding formulation, over entirely investigated period. The massive degradation in the *stage I* was mainly attributed to the cleavage of the O-C bonds between alternative N-acetyl sites under the Lysozyme action leading to the remove of some chitosan chains and dissolution of some chitosan oligomers. This correlates well with the rapid swelling of the matrix, which facilitated the enzyme access to the suitable sites. Further, the slow degradation in the *stage II*, was attributed mainly to the erosion by dissolution of the chitosan chains favored by the reversible imine units which break the crosslinking nodes. The more accelerated degradation in *the stage III* compared to the *stage II* can be attributed to an erosion rush, favored by the defects produced into the matrix in the first two degradation stages. The degradation was more accentuated for the formulations compared to the reference matrix, due to the supplementary defects created by ***DCF*** release. Analyzing these data, it can be concluded that the biodegradation of the investigated samples was a result of two concomitant effects: (i) the cleavage of the O-C bonds between alternative N-acetyl sites under the Lysozyme effect, and (ii) erosion by dissolution of the chitosan chains favored by the reversible imine units which break the crosslinking nodes [51]. This assessment was persistent with SEM microphotographs acquired over the degradation period. Despite the high mass loss, no evident shape differences were observed, suggesting that the biodegradation occurred in the entire volume of the samples and not only at the surface. SEM microphotographs indeed showed the destruction of the microstructure by erosions of the pore walls, whose aspect transformed from smooth to rough (Fig. 7a,b). Moreover, even breaks of the pore walls were noted (Fig. 7c,d).

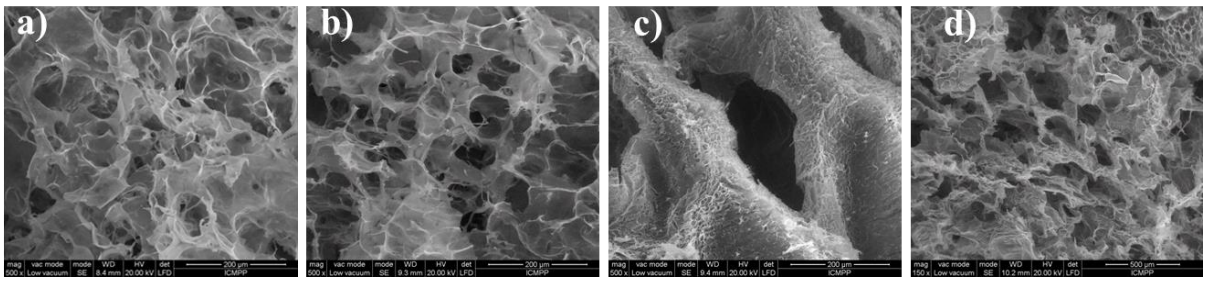

Fig.7. SEM microphotographs of some representative formulations acquired over the degradation period, a) **CSD2** after first day; b) **CSD2** after 3 day; c) **CS1.5** after 21 days; d) **CS2P** after 21 days

3.6. In *vitro* release study

The main goal of this paper was to investigate the ability of the salicyl-imine-chitosan hydrogels to act as matrix for prolonged drug release systems. To this aim, the *in vitro* drug release profile was analyzed for the **CSD1.5** and **CSD2** formulations, which demonstrated the most appropriate properties [30]. As can be seen in Fig. 8, the release profile is slightly different for the two samples, reflecting the influence of the crosslinking density and consequently of the pore size. Thus, in the first 8 hours, a higher release rate was noted in the case of **CSD1.5**, for which the percent of drug released was 33% compared to 25% for **CSD2**. This can be correlated with the presence of drug crystals of larger dimensions, less anchored into the matrix and so more prone to dissolution. Their occurrence was the most probably facilitated by higher viscosity of the **CSD1.5** system during hydrogelation, as also observed for other systems [22]. Further, the drug release proceeded in a sustained manner for both samples, reaching an almost equal percent around 70%, in the day 10. In this stage, the release rate appeared to be higher for **CSD2**, the most probably correlated to the lower crosslinking density and lower density of the larger pores, which facilitated the faster drug diffusion. Interesting enough, while for the **CSD2** no significant ***DCF*** release was further noted, the prolonged release continued from **CSD1.5**, reaching 91 % in the day 22 (Table S3). Compared to other chitosan based formulations, it can be remarked that the *in situ* hydrogelation in the presence of the drug led to a good equilibrium between a moderate burst release in the first 8 hours and a prolonged release of the drug in the next 10 days, appropriate for the design of the controlled drug release systems (Table 2) [4]. The *in situ* crosslinking led to strong physical forces between the drug molecules and the matrix, overcoming the disadvantage of a pronounced burst release and assuring a sustained prolonged delivery of the drug. A synthetic view on the main parameters which influences the drug release, i.e. swelling and biodegradation, evidences that the drug release profile was quite similar with that of the biodegradation one, a benefic aspect for real bioapplications.

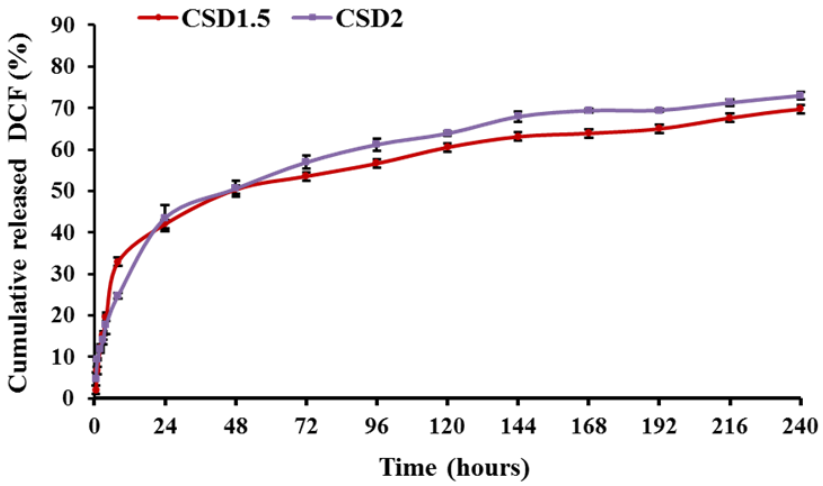

Fig. 8. *In vitro* cumulative ***DCF*** release profiles from **CSD1.5** and **CSD2** formulations

Tabel 2. Release parameters of ***DCF*** from different chitosan based materials

Materials	Release parameters	Reference
DCF *in situ* loaded into salicyl-imine-chitosan hydrogels	Burst release: 25-33% (8h), prolonged release: 70% (10 days) pH=7.4	present study
DCF *in situ* loaded into nitrosalicyl-imine-chitosan hydrogels	Burst release: 20-50% (8h), prolonged release: 90% (8 days) pH=7.4	[23]
DCF *in situ* loaded into chitosan/Hyaluronic acid/glutaraldehyde hydrogels	Burst release: around 50% (8h), prolonged release: 100% (24h) pH=7.2	[36]
3D plotted alginate fibres embedded with ***DCF*** and bone cells coated with chitosan	Burst release: 90% (8h), prolonged release: 100% (24-50h) pH=7.2	[3]
DCF *in situ* loaded in Cross-Linked Chitosan-Tricarballylic Acid Hydrogels	Burst release: around 20 % (8h), prolonged release: 8% to 67% (96h) pH= 5.5	[37]
DCF *in situ* loaded into chitosan/silk fibroin films	Burst release: 65.1% (10 min), pH=7.2	[28]
DCF adsorbed into alginate/carboxymethyl chitosan -ZnO hydrogel beads	Burst release: 30-50% (4h), prolonged release: 100% (8h) pH=7.4	[35]
DCF adsorbed into hydrogels beads based on chitosan-g-poly(acrylicacid)/attapulgite/sodium alginate	Burst release: around 40-90% (8h), prolonged release: 100% (24h) pH=7.4	[29]
DCF entrapped by ionic interaction into chitosan micro/nanoparticles	Burst release: 85 % (10 min), prolonged release: 100% (3h) pH=7.4	[31]
DCF adsorbed into chitosan graft with different comonomers	Burst release: 62-98% (5h), prolonged release: 85-99% (24h) pH=7.4	[34]

3.7. Analysis of *in vitro DCF* release kinetics

For a more complex view on the mechanism of ***DCF*** release from the salicyl-imine-chitosan matrix, five different mathematic models, *zero order*, *first order*, *Higuchi*, *Hixson–Crowell* and *Korsmeyer-Peppas*, were fitted on the two stages of the release profile (Table 3, Fig.S2) [39, 40, 57]

Table 3. Results of the fitting of the release curves on different mathematical models

Model	***Zero Order***		***First Order***		***Higuchi***		***Korsmeyer-Peppas***			***Hixson-Crowell***	
Code	R^2	K_0	R^2	K	R^2	K_H	R^2	K	n	R^2	K
CSD1.5*	0.994	3.7	0.998	0.05	0.994	14.2	0.997	0.15	0.75	0.997	-0.07
CSD2*	0.985	2.2	0.990	0.03	0.989	8.6	0.982	0.11	0.47	0.988	-0.04
CSD1.5**	0.950	0.18	0.970	0.004	0.983	2.9	0.991	0.05	0.22	0.970	-0.005
CSD2**	0.970	0.21	0.985	0.005	0.994	3.5	0.997	0.05	0.25	0.980	-0.006

*First stage =1h-8h; ** Second stage = 1 day- 5days

For the *first release* stage, the graphical representation of the five mathematical models gave a high correlation coefficient (R^2=0.982-0.998), indicating a complex mechanism of ***DCF*** delivery, governed by many factors, as follows. The fitting of the ***Zero order model***, which reflects the dissolution of the drug as a function of time, correlates with the fast swelling of the formulations in the first 8 hours, which favours the ***DCF*** solubilisation. The lower release constant of the formulation with lower crosslinking degree, **CSD2**, is unusual among drug release formulations [23]. It can be explained by a more intimate mixing of the ***DCF*** molecules into the matrix during the *in situ* hydrogelation, resulting in a stronger anchoring by physical forces. ***Higuchi*** model indicates that diffusion of the ***DCF*** molecules through the matrix play an important role in the drug release process. The higher proportionality constant in the case of **CSD1.5** indicates an easier diffusion of the drug molecules through the matrix. This correlates well with the faster degradation rate, which produced defects into the matrix facilitating the diffusion process. The influence of matrix erosion by biodegradation on the ***DCF*** diffusion through it, was further confirmed by the fitting of the ***Hixson-Crowell model***. A clearer difference on the influence of the matrix on the drug diffusion was done by the fitting of the **Korsmeyer-Peppas** model. As can be seen in table 3, the value of the diffusional exponent, n, is comprised in the 0.47- 0.75 range, indicating a non-Fickian anomalous transport when the diffusion through the matrix was occurring simultaneously with the matrix swelling/erosion [58]. However, the lower value of n in the case of **CSD2** indicates the preponderant influence of the diffusion on release kinetics, while the higher value in the case of **CSD1.5** is in line with

a substantial influence of the matrix erosion [40]. The fitting of the *first order model* indicate that the amount of ***DCF*** released is also dependent by that encapsulated into matrix.

A good fitting of the models on the release data was obtained in the *second stage*, too. Compared to the *first stage*, it was noted a slight decrease of the correlation coefficients, in agreement with a deeper change of the matrix over time. The most significant decrease was obtained for the fitting of the *first order model* on the release data of **CSD1.5** (R^2=0.95), according to a diminishing of the role of ***DCF*** dissolution on the release. A decrease of the proportionality constants and almost an equalization of their values were noted too, according to a slower release with almost equal velocity of the ***DCF*** through the two matrixes. In this line, a significant change was noted for the diffusional coefficient n, which fell to values under 0.47, indicating that the non-Fickian diffusion in the *first stage* turned into Fickian diffusion in the *second stage*. This means that the diffusion of the ***DCF*** molecules through the matrix is mainly controlled by the concentration gradient and less by the matrix.

Analyzing these data it can be envisaged that the drug release mechanism was mainly controlled by the state of the drug into the matrix, which is controlled by the hydrogelation speed. Thus, for the **CSD1.5**, whose hydrogelation occurred faster giving a more viscous system, the drug was most probably encapsulated as bigger crystals. They were less anchored into the matrix and more prone to a faster dissolution in the *first stage*, followed by a prolonged release up to almost totally. On the other hand, a slower hydrogelation for the **CSD2** with lower crosslinking density, allowed a finer dispersion of the drug into the matrix, with a larger amount at molecular level, strongly anchored by physical forces and less prone to dissolution. This led to a slower release in the *first stage* and a lower amount of the totally drug delivered.

3.8. In vivo biocompatibility

The formulations reported in this paper were designed based on natural originating reagents, with good chances to be applied for *in vivo* applications. In this line of thought, the next step of their study was the investigation of the *in vivo* biocompatibility on experimental rats. To this end, the hemodynamic, immune and biochemical profile of the animals implanted with the formulations and the corresponding xerogels were measured during an observation period of 7 days. None of the animals died over the investigation period. The clinical monitoring of the tested groups did not reveal significant modifications of the animal`s general status, suggesting no toxic effect of these formulations. No behavioural deviations such as reduced food uptake, abnormal posture, spontaneous motor activity disturbances or lethargy were noted in the rats treated with **CS1.5**, **CSD1.5**, **CS2** and **CSD2**. Compared to control animals, no

substantial variations in the percentage of the leucocytes formula elements were observed after administration (1 or 7 days), indicating their safety hematologic profile *in vivo* (Fig. 9). The considered biochemical parameters, such as: ALT, AST, and LDH activity (Fig.10), the blood level of uric acid and creatinine (Fig. 11) were found to be normal in implanted rats, at the same level as for control, attesting the lack of toxicity to liver and kidney, respectively.

The assessment of the immune defence capacity, did not revealed major differences in the phagocytic capacity of peripheral neutrophils and the serum complement activity (Fig.12), between the rats with ***DCF*** pellets and the groups receiving formulations and corresponding implants, suggesting that they did not disturb the animal`s normal immune response [59].

All these data showed that in the experimental conditions of subcutaneous implantation of pellets of **CS1.5**, **CSD1.5**, **CS2**, **CSD2** displayed a good *in vivo* biocompatibility in rats, suggesting that, they represent valuable materials for biomedical devices.

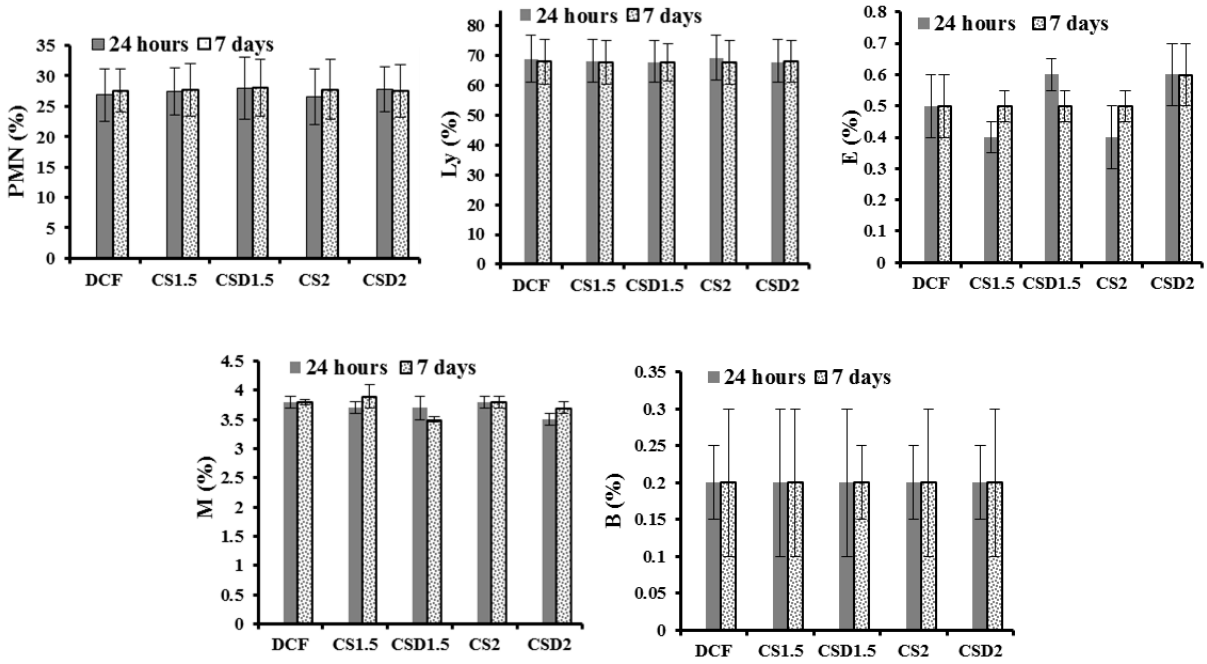

Fig. 9. Differential white cell count in rats with ***DCF***, **CS1.5**, **CSD1.5**, **CS2** and **CSD2** pellets. Values were presented as mean ± S.D. of mean for 6 rats in a group.

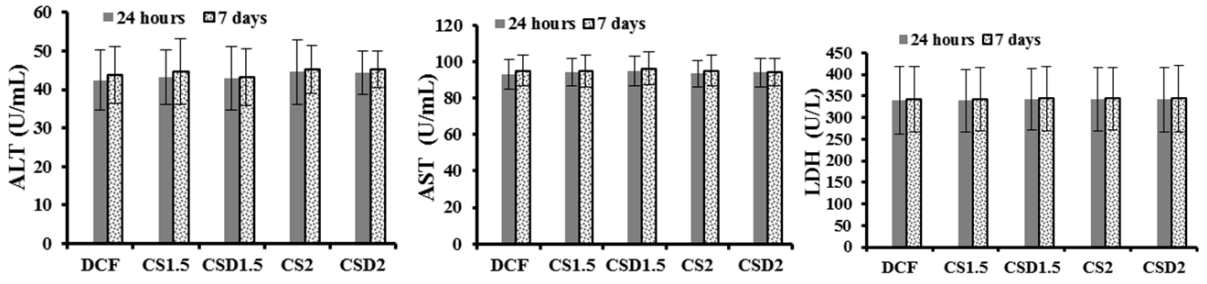

Fig.10. GOT, GPT, LDH activity in rats with ***DCF*, CS1.5, CSD1.5, CS2, CSD2** pellets. Values were presented as mean ± S.D. of mean for 6 rats in a group.

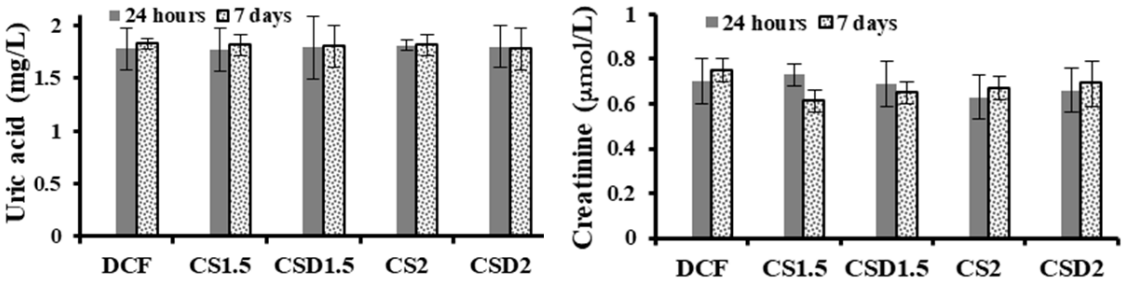

Fig. 11.Creatinine and uric acid values in rats with ***DCF*, CS1.5, CSD1.5, CS2** and **CSD2** pellets. Values were presented as mean ± S.D. of mean for 6 rats in a group.

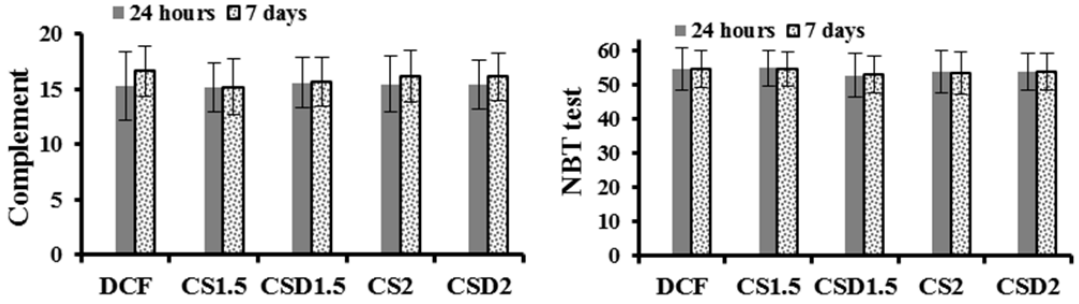

Fig.12. The phagocytic capacity of peripheral neutrophils and the serum complement activity in rats with ***DCF*, CS1.5**, **CSD1.5**, **CS2** and **CSD2** pellets. Values were presented as mean ± S.D. of mean for 6 rats in a group.

Conclusions

New formulations based on salicyl-imine-chitosan hydrogels were successfully prepared by *in situ* hydrogelation of chitosan with salicylaldehyde in the presence of the ***DCF*** model drug. By varying the molar ratio between the glucosamine units of chitosan and salicylaldehyde was yielded a series of four formulations with different crosslinking degrees. FTIR, X-ray diffraction, SEM and POM microscopy proved that the hydrogelation process was governed by the formation of the imine linkages and their supramolecular ordering, while ***DCF*** was anchored in the hydrogel matrix at submicrometric level, by physical interactions. The formulations revealed a porous morphology, which respects the general rule proved for hydrogels: the diameter of the interconnected pores progressively increased as the crosslinking degree decreased. The formulations showed a fast swelling, reaching an *in vitro* maximum swelling degree around 20-28 g/g in less than 2 hours, significant higher compared to the reference xerogels which showed a maximum swelling degree of 13-16 g/g. The *in vitro* enzymatic degradation occurred in three stages, as result of the Lysozyme effect and erosion

by dissolution of the chitosan chains. The release profile of the formulations proceeded in a controlled manner, exhibiting a burst effect of 33% in the first 8 hours and a prolonged release up to 70% within 10 days, correlated to the state of the drug into the matrix and the hydrogelation speed. The *in vivo* tests showed that the hemodynamic, immune and biochemical profiles of the experimental rats implanted with the formulations and corresponding hydrogels were similar with that of the control animals, indicating an excellent *in vivo* biocompatibility. In the light of these findings it can be affirmed that these new formulations can be promising materials for biomedical applications.

Acknowledgements

The research leading to these results has received funding from the Romanian National Authority for Scientific Research, MEN-UEFISCDI grant, project number PN-III-P1-1.2-PCCDI2017-0569 (10PCCDI/2018) and the European Commission through the project H2020-MSCA-RISE-2019,
SWORD- DLV-873123.

References

[1] D. Liu, F. Yang, F. Xiong, N. Gu, The Smart Drug Delivery System and Its Clinical Potential, Theranostics. 6 (2016) 1306–1323. https://doi.org/10.7150/thno.14858.

[2] S.G. Kumbar, A.R. Kulkarni, M. Aminabhavi, Crosslinked chitosan microspheres for encapsulation of diclofenac sodium: effect of crosslinking agent, J. Microencapsulation. 19 (2002) 173-180. https://doi.org/10.1080/02652040110065422.

[3] H.-Yi Lin, T.-W. Chang, T.-K. Peng, Three-dimensional plotted alginate fibers embedded with diclofenac and bone cells coated with chitosan for bone regeneration during inflammation, J. Biomed. Mater Res. A. 106 (2018) 1511-1521. https://doi.org/10.1002/jbm.a.36357.

[4] K. Matsumura, 2020. Nanocomposite Hydrogels for Biomedical Applications. Appl. Sci. 10, 389. https://doi.org/10.3390/app10010389.

[5] G. Dalei, S. Das, S.P. Das, Non-thermal plasma assisted surface nanotextured carboxymethyl guar gum/chitosan hydrogels for biomedical applications, RSC Adv. 9 (2019) 1705-1716. https://doi.org/10.1039/C8RA09161G.

[6] A. Singh, N.A. Peppas, Hydrogels and Scaffolds for Immunomodulation, Adv. Mater. 26 (2014) 6530–6541. https://doi.org /10.1002/adma.201402105.

[7] A.S. Hoffman, Hydrogels for biomedical applications, Adv. Drug Deliv. Rev. 64 (2012) 18–23. https://doi.org/10.1016/j.addr.2012.09.010.

[8] Q. Chai, Y. Jiao, X. Yu, 2017. Hydrogels for Biomedical Applications: Their Characteristics and the Mechanisms behind Them. Gels. 3, 6 https://doi.org/10.3390/gels3010006.

[9] A. Sosnik, K.P. Seremeta, 2017. Polymeric Hydrogels as Technology Platform for Drug Delivery Application. Gels 3, 25. https://doi.org/10.3390/gels3030025.

[10] K.S.V. Krishna Rao, B.V.K. Naidu, M.C.S. Subha, M. Sairam, T.M. Aminabhavi, Novel chitosan-based pH-sensitive interpenetrating network microgels for the controlled release of cefadroxil, Carbohydr. Polym. 66 (2006) 333–344. https://doi.org/10.1016/j.carbpol.2006.03.025.

[11] S. Dreve, I.Kacso, I.Bratu, E. Indrea, 2009. Chitosan-based delivery systems for diclofenac delivery: preparation and characterization. J. Phys.: Conf. Ser. 182, 012065. https://doi.org/10.1088/1742-6596/182/1/012065.
[12] S. Hua, H. Yang, W. Wang, A. Wang, Controlled release of ofloxacin from chitosan-montmorillonite hydrogel, Appl. Clay. Sci. 50 (2010) 112-117. https://doi.org/10.1016/j.clay.2010.07.012.
[13] C.-L. Savin, M. Popa, C. Delaite, M.Costuleanu, D. Costin, C.A. Peptu, Chitosan grafted-poly(ethyleneglycol) methacrylate nanoparticles as carrier for controlled release of bevacizumab, Mat. Sci. Eng. C Mater. 98 (2019) 843-860. https://doi.org/10.1016/j.msec.2019.01.036.
[14] J. Varshosaz, M. Tabbakhian, Z. Salmani, Designing of a Thermosensitive Chitosan/Poloxamer *In Situ* Gel for Ocular Delivery of Ciprofloxacin, Open Drug Deliv. J. 2 (2008) 61–70. https://doi.org/10.2174/1874126600802010061.
[15] Q. Guo, C. Liu, B. Hai, T. Ma, W. Zhang, J. Tan, X. Fu, H.Wang, Y. Xu, C. Song, Chitosan conduits filled with simvastatin/Pluronic F-127 hydrogel promote peripheral nerve regeneration in rats, J. Biomed. Mater. Res. B Appl. Biomater. 106 (2017) 787-799. https://doi.org/10.1002/jbm.b.33890.
[16] L. Elviri, A. Bianchera, C. Bergonzi, R. Bettini, Controlled local drug delivery strategies from chitosan hydrogels for wound healing, Expert Opin. Drug Deliv. 14 (2017) 897-908. https://doi.org/10.1080/17425247.2017.1247803.
[17] A. Islam, R.T. Yasin, Structural and viscoelatic properties of chitosan-based hydrogels and its drug delivery application, Int. J. Biol. Macromol. 59 (2013) 119-124. https://doi.org/10.1016/j.ijbiomac.2013.04.044.
[18] M.M. Iftime, S. Morariu, L. Marin, Salicyl- imine-chitosan hydrogels: Supramolecular architecturing as a crosslinking method toward multifunctional hydrogels, Carbohydr. Polym. 165 (2017) 39-50. https://doi.org/10.1016/j.carbpol.2017.02.027.
[19] A.M Craciun, L. Mititelu Tartau, M. Pinteala, L. Marin, Nitrosalicyl-imine-chitosan hydrogels based drug delivery systems for long term sustained release in local therapy, J. Colloid Interface Sci. 536 (2019) 196-207. https://doi.org/10.1016/j.jcis.2018.10.048.
[20] M.M. Iftime, L. Marin, Chiral betulin- imino-chitosan hydrogels by dynamic covalent sonochemistry, Ultrason. Sonochem. 45 (2018) 238-247. https://doi.org/10.1016/j.ultsonch.2018.03.022.
[21] L. Marin, D. Ailincai, M. Mares, E. Paslaru, M. Cristea, V. Nica, B.C. Simionescu, Iminochitosan biopolymeric films. Obtaining, self-assembling, surface and antimicrobial properties. Carbohydr. Polym. 117 (2015) 762-770. https://doi.org/10.1016/j.carbpol.2014.10.050.
[22] D. Ailincai, L. Mititelu Tartau, L. Marin, Drug delivery systems based on biocompatible imino-chitosan hydrogels for local anticancer therapy, Drug Deliv. 25 (2018) 1080-1090. https://doi.org/10.1080/10717544.2018.1466937.
[23] A.M. Olaru, L. Marin, S. Morariu, G. Pricope, M. Pinteala, L. Tartau-Mititelu, Biocompatible based hydrogels for potential application in local tumour therapy, Carbohydr. Polym. 179 (2018) 59-70. https://doi.org/10.1016/j.carbpol.2017.09.066.
[24] D. Ailincai, L. Marin, S. Morariu, M. Mares, A.C. Bostanaru, M. Pinteala, B.C. Simionescu, M. Barboiu, Dual crosslinked iminoboronate-chitosan hydrogels with strong

antifungalactivity against Candida planktonic yeasts and biofilms, Carbohydr. Polym. 152 (2016) 306-316. https://doi.org/10.1016/j.carbpol.2016.07.007.
[25] L. Marin, D. Ailincai, S. Morariu, L. Tartau-Mititelu, Development of biocompatible glycodynameric hydrogels joining two natural motifs by dynamic constitutional chemistry, Carbohydr. Polym. 170 (2017) 60-71. https://doi.org/10.1016/j.carbpol.2017.04.055.
[26] A. Bejan, D. Ailincai, B.C. Simionescu, L. Marin, Chitosan hydrogelation with a phenothiazine based aldehyde – toward highly luminescent biomaterials, Polym. Chem. 9 (2018) 2359-2369. https://doi.org/10.1039/C7PY01678F.
[27] J. Daneš, S. Kreft, Salicylaldehyde is a characteristic aroma component of buckwheat groats, Food Chem. 109 (2008) 293–298. https://doi.org/10.1016/j.foodchem.2007.12.032.
[28] R. Rujiravanit, S. Kruaykitanon, A.M. Jamieson, S. Tokura, Preparation of Crosslinked Chitosan/Silk Fibroin Blend Films for Drug Delivery System, Macromol. Biosci. 3 (2003) 604–611. http://dx.doi.org/10.1002/mabi.200300027.
[29] Q. Wanga, J. Zhang, A. Wang, Preparation and characterization of a novel pH-sensitive chitosan-g-poly(acrylic acid)/attapulgite/sodium alginate composite hydrogel bead for controlled release of diclofenac sodium, Carbohydr. Polym. 78 (2009) 731–737. http://dx.doi.org/10.1016/j.carbpol.2009.06.010.
[30] K. S. V. Krishna Rao, M. C. S. Subha et al. Synthesis, characterization and controlled release characteristics of PEGylated hydrogels for diclofenac sodium, Des. Monomers Polym. 9 (2006) 261-273. http://dx.doi.org/10.1163/156855506777350992.
[31] Y. Boonsongrit, A.Mitrevej, B.W. Mueller, Chitosan drug binding by ionic interaction, Eur. J. Pharm. Biopharm. 62 (2006) 267–274. http://dx.doi.org/10.1016/j.ejpb.2005.09.002.
[32] H. Hosseinzadeh, Controlled release of diclofenac sodium from pH-responsive carrageenan-g-poly(acrylic acid) superabsorbent hydrogel, J. Chem. Sci. 122 (2010) 651–659. https://doi.org/10.1007/s12039-010-0100-1.
[33] R. Kozakevych, Y. Bolbukh, V. Tertykh, Controlled Release of Diclofenac Sodium from Silica-Chitosan Composites, WJNSE. 3 (2013) 69-78. https://doi.org/10.4236/wjnse.2013.33010.
[34] R.K. Sharma, Lalita, A.P. Singh, G.S. Chauhan, Grafting of GMA and some comonomers onto chitosan for controlled release of diclofenac sodium, Int. J. Biol. Macromol. 64 (2014) 368-376. https://doi.org/10.1016/j.ijbiomac.2013.12.028.
[35] B. Niu, J. Jia, H. Wang, S. Chen, W. Cao, J. Yan X. , Gong, X. Lian, W. Li, Y.Y. Fan, In vitro and in vivo release of diclofenac sodium-loaded sodium alginate/carboxymethyl chitosan-ZnO hydrogel beads, Int. J. Biol. Macromol. 141 (2019) 1191-1198. https://doi.org/10.1016/ j.ijbiomac.2019.09.059.
[36] A. Abou-Okeil, A.A. Aly, A. Amr, A.A.F. Soliman, Biocompatible hydrogel for cartilage repair with adjustable properties, Polym. Adv. Technol. 30 (2019) 2026–2033. https://doi.org/10.1002/pat.4635.
[37] N. Igesias, E. Galbis, C. Valencia, M.V. De-Paz, J. A. Galbis, 2018. Reversible pH-Sensitive Chitosan-Based Hydrogels. Influence of Dispersion Composition on Rheological Properties and Sustained Drug Delivery. Polymers. 10, 392 https://doi.org/ 10.3390/polym10040392.
[38] P. Samoila, L. Sacarescu, A.I. Borhan, D. Timpu, M. Grigoras, N.Lupu, M. Zaltariov, V. Harabagiu, Magnetic properties of nanosized Gd doped Ni–Mn–Cr ferrites prepared using

the sol–gel autocombustion technique, J. Magn. Magn. Mater. 378 (2015) 92-97. https://doi.org/10.1016/j.jmmm.2014.10.174.
[39] P.L. Ritger, N.A. Peppas, A simple equation for description of solute release I. Fickian and non-Fickian release from non-swellable devices in form of slabs, sphere, cylinders or discs, J. Control. Release. 5 (1987) 23–36. https://doi.org/10.1016/0168-3659(87)90034-4.
[40] L. Masaro, X.X. Zhu, Physical models of diffusion for polymer solutions, gels and solids, Prog. Polym. Sci. 24 (1999) 731–775. https://doi.org/10.1016/S0079-6700(99)00016-7.
[41] S. Parasuraman, R. Raveendran, R. Kesava, Blood sample collection in small laboratory animals, J. Pharmacol. Pharmacother. 2 (2010) 87-93. https://doi.org/10.4103/0976-500X.72350.
[42] M.F. Wolf, J.M. Andwraon, Practical approach to blood compatibility assessments: general considerations and standards, in: Boutrand J-P edition, Biocompatibility and Performance of Medical Devices, Woodhead Publishing, 2012, pp.159-200, 201e-206e.
[43] X. Li, L. Wang, Y. Fan, Q. Feng, F.Z. Cui, 2012. Biocompatibility and toxicity of nanoparticles and nanotubes. J. Nanomater. 2012, 548389. https://doi.org/10.1155/2012/548389.
[44] Y. Onuki, U. Bhardwaj, F. Papadimitrakopoulos, D.J. Burgess, A review of the biocompatibility of implantable devices: current challenges to overcome foreign body response, J. Diabetes Sci. Technol. (2) 2008 1003-1015. https://doi.org/10.1177/193229680800200610.
[45] C. Gavrilovici, Introducere în bioetică, Editura Junimea, Iaşi, 2007.
[46] AVMA Guidelines on Euthanasia (Formerly Report of the AVMA Panel on Euthanasia), 2007 June, pp. 6-7.
[47] Directive 2010/63/EU of the European Parliament and of the Council of 22 September 2010 on the protection of animals used for scientific purposes.
[48] T. Maver, T.Mohan, L. Gradišnik, M.Finšgar, K.S. Kleinschek, U. Maver, (2019). Polysaccharide Thin Solid Films for Analgesic Drug Delivery and Growth of Human Skin Cells. Front. Chem. 7, 217. https://doi.org/10.3389/fchem.2019.00217.
[49] M.M. Iftime, G.L. Ailiesei, E. Ungureanu, L. Marin, 2019. Designing chitosan based ecofriendly multifunctional soil conditioner systems with urea controlled release and water retention. Carbohydr. Polym. 223, 115040. https://doi.org/10.1016/j.carbpol.2019.115040.
[50] P.B. Aieloa, F.A. Borgesa, K.M. Romeiraa, et al. Evaluation of Sodium Diclofenac Release Using Natural Rubber Latex as Carrier, Mat. Res. 17 (2014) 146-152. https://doi.org/10.1590/S1516-14392014005000010.
[51] Y. Song, N. Nagai, S. Saijo, H. Kaji, M. Nishizawa, T. Abe, In situ formation of injectable chitosan-gelatin hydrogels through double crosslinking for sustained intraocular drug delivery. Mater. Sci. Eng. C. 88 (2018) 1–12. https://doi.org/10.1016/j.msec.2018.02.022.
[52] L. Bi, Z. Cao, Y. Hu, Y. Song, L. Yu, B. Yang, J. Mu, Z. Huang, Y. Han, Effects of different cross-linking conditions on the properties of genipin-cross-linked chitosan/ collagen scaffolds for cartilage tissue engineering, J. Mater. Sci. Mater. Med. 22 (2011) 51–62. https://doi.org/10.1007/s10856-010-4177-3.
[53] W. Zhang, G. Ren, H. Xu, J. Zhang, H. Liu, S. Mu, X. Cai, T. Wu, 2016. Genipin cross-linked chitosan hydrogel for the controlled release of tetracycline with controlled release property, lower cytotoxicity, and long-term bioactivity, J. Polym. Res. 23, 156. https://doi.org/10.1007/s10965-016-1059-5.

[54] J. Xu, S. Strandman, J.X. Zhu, J. Barralet, M. Cerruti, Genipin-crosslinked catecholchitosan mucoadhesive hydrogels for buccal drug delivery, Biomaterials. 37 (2015) 395–404. https://doi.org/10.1016/j.biomaterials.2014.10.024.

[55] L. Marin, A. Zabulica, M. Sava, Symmetric liquid crystal dimers containing a luminescent mesogen: synthesis, mesomorphic behavior, and optical properties, Soft Material. 11 (2013) 32–39. https://doi.org/10.1080/1539445X.2011.567434

[56] K. Tomihata, Y. Ikada, *In vitro* and *in vivo* degradation of films of chitin and its deacetylated derivatives, Biomaterials. 18 (1997) 567-575. https://doi.org/10.1016/s0142-9612(96)00167-6.

[57] P. Treenate, P. Monvisade, In vitro drug release profiles of pH-sensitive hydroxyethylacryl chitosan/sodium alginate hydrogels using paracetamol as a soluble model drug, Int. J. Biol. Macromol. 99 (2017) 71-78. http://dx.doi.org/10.1016/j.ijbiomac.2017.02.061

[58] H. Tetsuo, K. Hideyoshi, Formulation study and drug release mechanism of a new theophylline sustained-release preparation, Int. J. of Pharm. 304 (2005) 91–101. http://dx.doi.org/10.1016/j.ijpharm.2005.07.022.

[59] C.K. Ferreira, J. Prestes, F.F. Donatto, R. Verlengia, J.W. Navalta, C.R. Cavaglieri, Phagocytic responses of peritoneal macrophages and neutrophils are different in rats following prolonged exercise, Clinics (Sao Paulo). 65 (2010) 1167-1173. http://dx.doi.org/10.1590/s1807-59322010001100020.